

Supporting Information

Thermal-insulating ceramic fiber aerogels reinforced fusing knots of overlapping fibers for superelasticity and high compression resistance

Xiaolin Meng,^{abc†} Cui Liu,^{b‡} Jixiang Zhang,^{*abc} Wei Guo,^{*bc} Nian Li,^{bc} Yang Chen,^{bce} Huan Xu,^{bcd} Min Xi,^{bc} Shudong Zhang^{*bc} and Zhenyang Wang^{*bc}

a School of Mechatronics and Vehicle Engineering, Chongqing Jiaotong University,
Chongqing 400074, China

b Institute of Solid State Physics, Hefei Institutes of Physical Science, Chinese
Academy of Sciences, Hefei, 230031, China.

c Key Laboratory of Photovoltaic and Energy Conservation Materials, Hefei Institutes
of Physical Science, Chinese Academy of Sciences, Hefei, 230031, China.

d University of Science and Technology of China, Hefei 230026, China.

e School of Materials Science and Engineering, Chongqing Jiaotong University,
Chongqing 400074, China

*Corresponding Authors

Email:zhangjixiang@163.com,weiguo@issp.ac.cn,sdzhang@iim.ac.cn,zywang@iim.
ac.cn

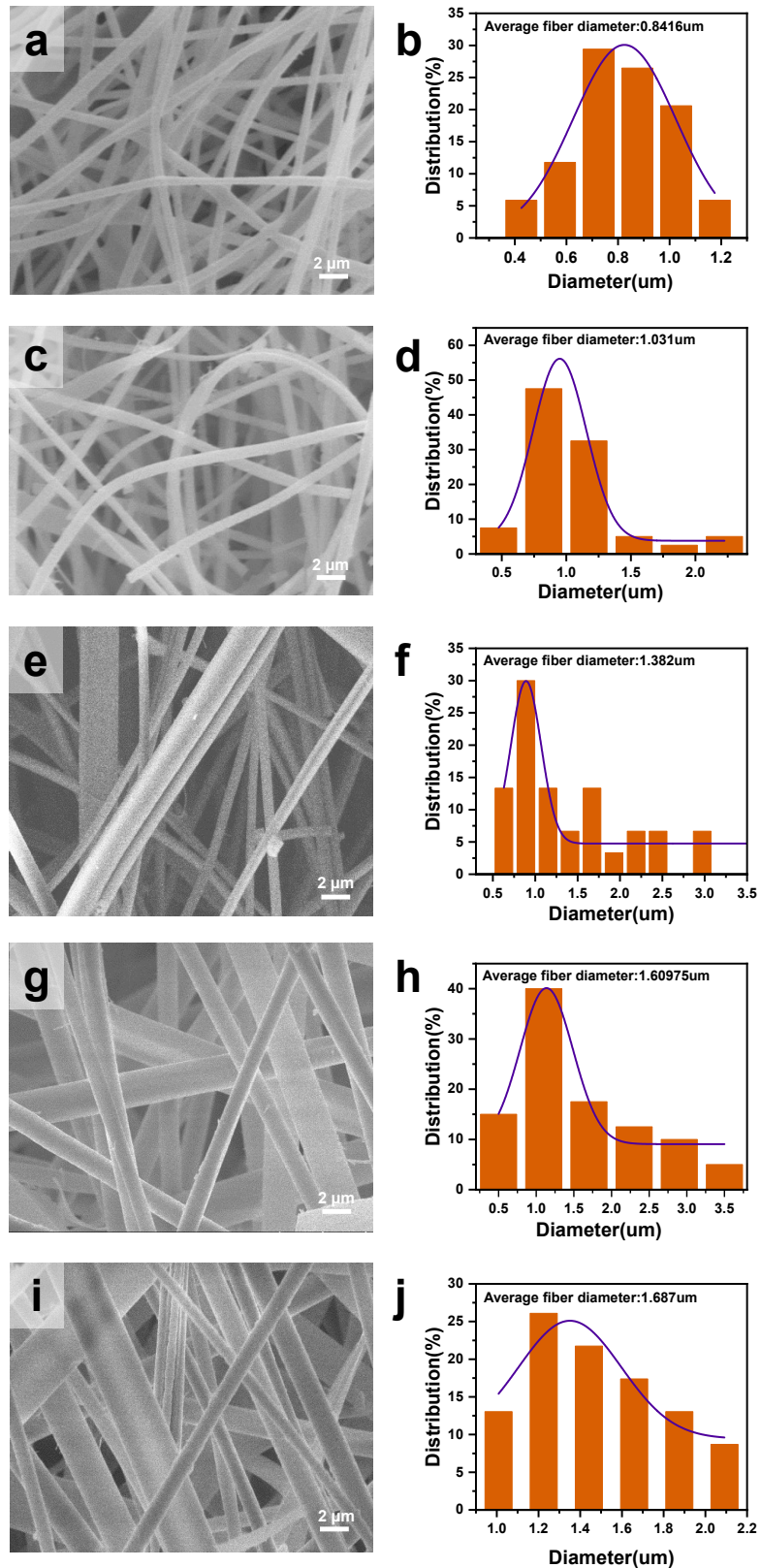


Fig. S1 The SEM images of the individual SiZrOC NFTs with the different molar ratio of silicon/zirconium and their corresponding diameter distributions.

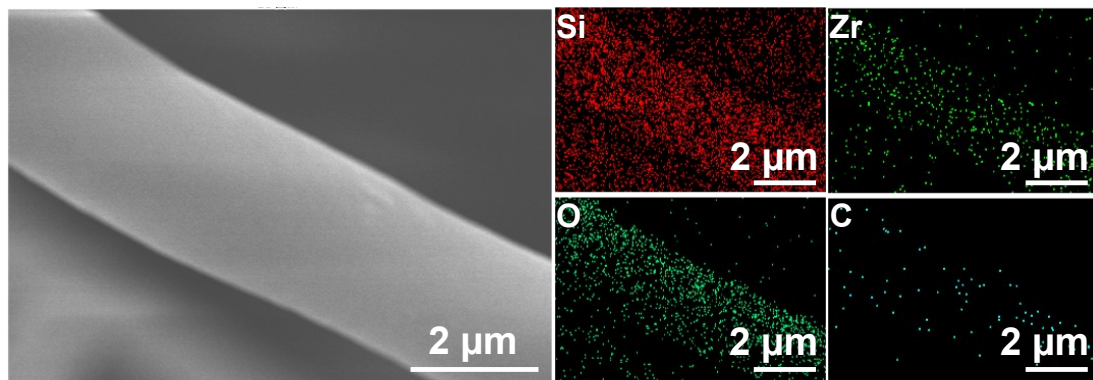


Fig. S2 EDS mapping of individual SiZrOC NFTs.

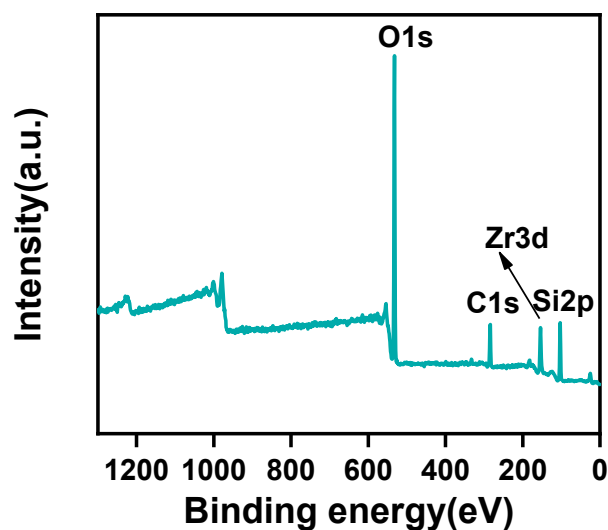


Fig. S3 The full XPS spectrum of individual SiZrOC NFTs.

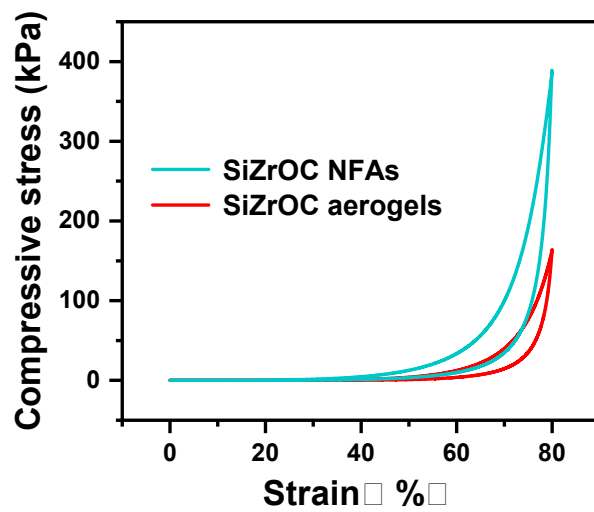


Fig. S4 Stress-strain curves of the macrobulk SiZrOC NFAs with ACP and SiZrOC fiber aerogels.
without ACP.

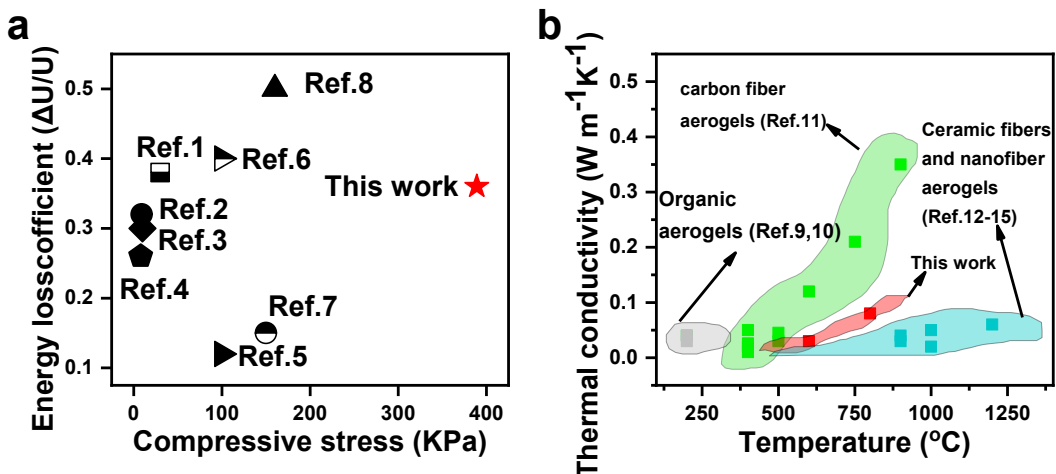


Fig. S5 (a)The maximum compressive strength of the aerogel in this study and other aerogels in previous studies at 80% strain and the material energy loss coefficient after long cycling, and (b) thermal conductivity versus temperature for different aerogel materials.

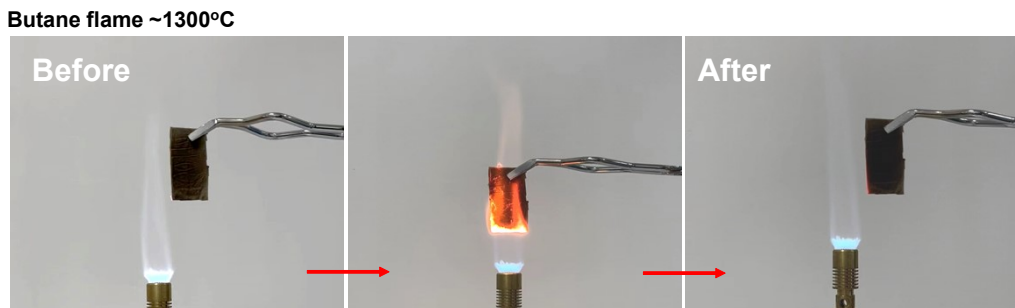


Fig. S6 Anti-temperature resistance of individual SiZrOC NFTs with fusing knots of ACP.

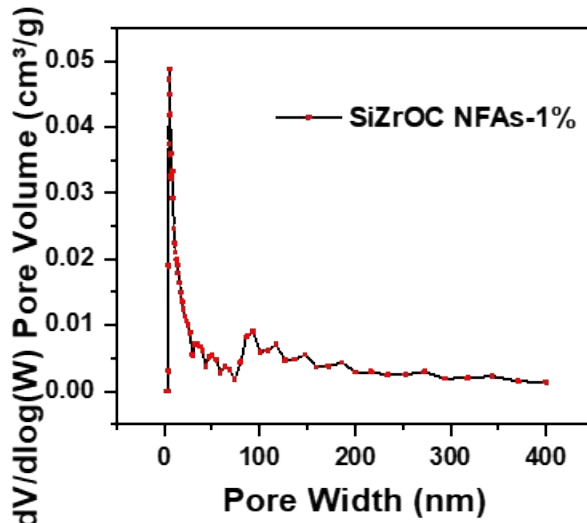


Fig. S7 Pore volume-pore size distribution of the macrobulk SiZrOC NFAs-1%.

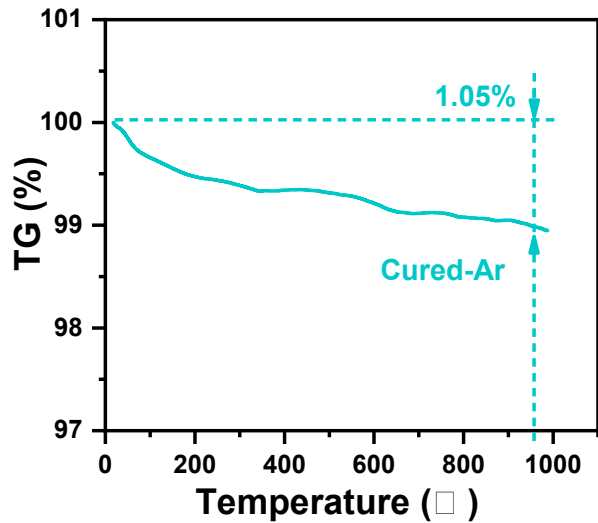


Fig. S8 Thermogravimetric analysis of the macrobulk SiZrOC NFAs.

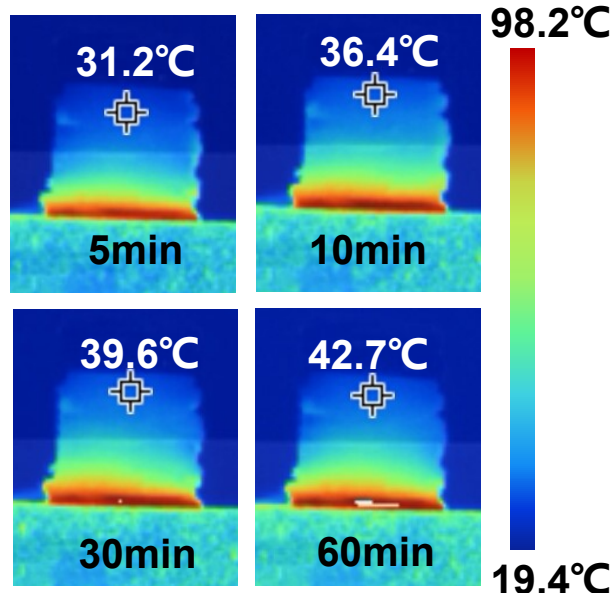


Fig. S9 Infrared images of the macrobulk SiZrOC NFAs with thickness of ~ 5 cm at different times under the thermal plate at 100°C.

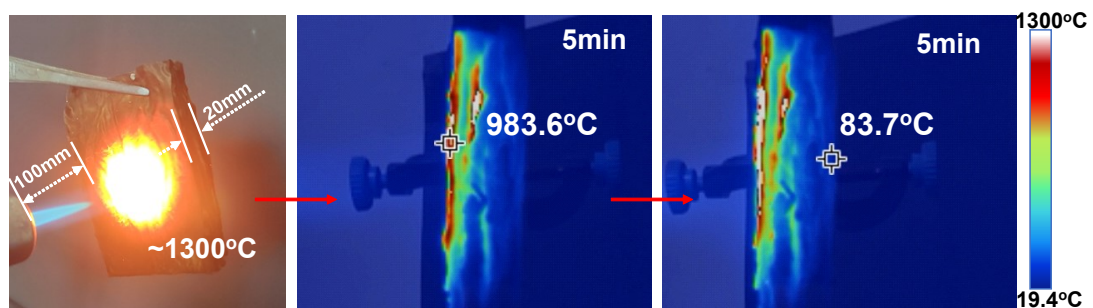


Fig. S10 Infrared image of the macrobulk SiZrOC NFAs under thermal shock of a butane flame at 1300°C.

References

- 1 L. Zhou, L. Wu, T. Wu, D. Chen, X. Yang, G. Sui, *Mater. Today Nano*, 2023, **22**, DOI:10.1016/j.mtnano.2023.100306.
- 2 L. Dou, X. Zhang, X. Cheng, Z. Ma, X. Wang, Y. Si, J. Yu and B. Ding, *ACS Appl. Mater.*, 2019, **11**, 29056-29064.
- 3 Y. Si, L. Dou, J. Yu, B. Ding, *Sci. Adv.*, 2018, **4**, DOI: 10.1126/sciadv.aas8925.
- 4 L. Dou, X. Zhang, H. Shan, X. Cheng, Y. Si, J. Yu, B. Ding, *Adv. Funct. Mater.*, 2020, **30**, DOI: 10.1002/adfm.202005928.
- 5 X. Zhang, X. Cheng, Y. Si, J. Yu, B. Ding, *ACS Nano*, 2022, **16**, 5487–5495.
- 6 X. Zhang, X. Cheng, Y. Si, J. Yu, B. Ding, *Chem. Eng. J.*, 2022, **433**, DOI:10.1016/j.cej.2021.133628.
- 7 B. Fan, L. Wu, A. Ming, Y. Liu, Y. Yu, L. Cui, M. Zhou, Q. Wang, P. Wang, *Int. J. Biol. Macromol*, 2023, **242**, DOI:10.1016/j.ijbiomac.2023.125066.
- 8 H. Wang, L. Cheng, J. Yu, Y. Si, B. Ding, *Nat Commun*, 2024, **336**, DOI: 10.1038/s41467-023-44657-2.
- 9 L. Zuo, Y. Zhang, L. Zhang, Y. Miao, W. Fan, T. Liu, *Materials*, 2015, **8**, 6806–6848.
- 10 J. Wu, W. Sung, H. Chu, *Int. J. Heat Mass Transf.*, 1999, **42** 2211–2217.
- 11 J. Ma, J. Li, P. Guo, S. Pang, C. Hu, R. Zhao, S. Tang, H. Cheng, *Carbon*, 2022, **196**, 807-818.
- 12 G. Zu, J. Shen, L. Zou, W. Wang, Y. Lian, Z. Zhang, A. Du, *Chem. Mater.*, 2013, **25** 4757–4764.
- 13 Z. Li, L. Gong, X. Cheng, S. He, C. Li, H. Zhang, *Mater. Des.*, 2016, **99**, 349–355.
- 14 H. Zheng, H. Shan, X. Wang, L. Liu, J. Yu, B. Ding, *RSC Adv.*, 2015, **5**, 91813–91820.

15 D. Zong, W. Bai, X. Yin, J. Yu, S. Zhang and B. Ding, *Adv. Funct. Mater*, 2023,
33, DOI: 10.1002/adfm.202301870.